Research Paper

Brain network structural connectome abnormalities among youth with attention-deficit/hyperactivity disorder at varying risk for bipolar I disorder: a cross-sectional graph-based magnetic resonance imaging study

Ziyu Zhu, PhD*; Du Lei, PhD*; Kun Qin, PhD; Xiuli Li, PhD; Wenbin Li, PhD; Maxwell J. Tallman, BS; L. Rodrigo Patino, MD, MsC; David E. Fleck, PhD; Veronica Aghera, BS; Qiyong Gong, MD, PhD; John A. Sweeney, PhD; Robert K. McNamara, PhD; Melissa P. DelBello, MD, MS

Background: Attention-deficit/hyperactivity disorder (ADHD) is highly prevalent among youth with or at familial risk for bipolar-I disorder (BD-I), and ADHD symptoms commonly precede and may increase the risk for BD-I; however, associated neuropathophysiological mechanisms are not known. In this cross-sectional study, we sought to investigate brain structural network topology among youth with ADHD, with and without familial risk of BD-I. **Methods:** We recruited 3 groups of psychostimulant-free youth (aged 10–18 yr), namely youth with ADHD and at least 1 biological parent or sibling with BD-I (high-risk group), youth with ADHD who did not have a first- or second-degree relative with a mood or psychotic disorder (low-risk group) and healthy controls. We used graph-based network analysis of structural magnetic resonance imaging data to investigate topological properties of brain networks. We also evaluated relationships between topological metrics and mood and ADHD symptom ratings. **Results:** A total of 149 youth were included in the analysis (49 healthy controls, 50 low-risk youth, 50 high-risk youth). Low-risk and high-risk ADHD groups exhibited similar differences from healthy controls, mainly in the default mode network and central executive network. We found topological alterations in the salience network of the high-risk group, relative to both low-risk and control groups. We found significant abnormalities in global network properties in the high-risk group only, compared with healthy controls. Among both low-risk and high-risk ADHD groups, nodal metrics in the right triangular inferior frontal gyrus correlated positively with ADHD total and hyperactivity/impulsivity subscale scores. **Limitations:** The cross-sectional design of this study could not determine the relevance of these findings to BD-I risk progression. **Conclusion:** Youth with ADHD, with and without familial risk for BD-I, exhibit common regional abnormalities in the brain connectome compared with healthy youth, whereas alterations in the salience network distinguish these groups and may represent a prodromal feature relevant to BD-I risk.

Introduction

Bipolar-I disorder (BD-I) is associated with premature functional disability and mortality.[1] The initial onset of BD-I frequently occurs during the peripubertal period[2] and is often preceded by symptoms of inattention and attention-deficit/hyperactivity disorder (ADHD).[3] The prevalence of ADHD[4] and BD-I[5] is higher among youth with a first-degree relative with BD-I, and converging evidence suggests that the combination of ADHD and familial risk for BD-I increases risk for BD-I.[6,7] However, the central pathoetiological mechanisms associated with the risk of developing BD among youth with ADHD remain poorly understood.

Structural and functional imaging studies indicate that youth with ADHD exhibit abnormalities in distributed neural systems associated with attention and cognitive processing,

Correspondence to: D. Lei, College of Medical Informatics, Chongqing Medical University, 1 Yixueyuan Road, Yuzhong District, Chongqing 400016, China; alien18@163.com. Q. Gong, Department of Radiology, West China Xiamen Hospital of Sichuan University, Xiamen, Fujian, China; qiyonggong@hmrrc.org.cn

*Ziyu Zhu and Du Lei contributed equally to this study.

Submitted Nov. 15, 2022; Revised Apr. 10, 2023; Revised May 29, 2023; Accepted May 30, 2023

Cite as: *J Psychiatry Neurosci* 2023 August 29;48(4). doi: 10.1503/jpn.220209

including the frontal lobe, parietal lobe, thalamus and putamen.[8,9] Existing evidence also suggests that functional and structural deficits in the frontal lobe and thalamus are associated with the emergence of ADHD,[10,11] and that maturation of the frontal cortex is associated with reductions in severity of ADHD symptoms.[12] Although alterations in the frontotemporal cortex and subcortical regions have been observed among youth at high genetic risk of BD-I,[13,14] little research has attempted to identify distinguishing brain features in youth with ADHD, with and without familial risk of BD-I.

The human brain connectome is composed of a complex and integrated set of connections and connected hubs that confer specialized and modular processing in a distributed or integrated manner.[15,16] Graph theoretical analysis, a connectome-based approach, quantifies brain network integration and segregation at the global and local (nodal) levels.[15] Specifically, the brain is modelled as a network composed of a number of nodes and edges, wherein nodes represent individual cortical and subcortical regions and edges reflect connectivity among nodes. The combination of highly connected hubs and short path length confers the capability for both specialized and modular processing in a distributed or integrated manner. Connectome analysis can assess network efficiency, clustering, modularity and path lengths between regions. This connectome-based approach has been widely used to characterize functional and structural network abnormalities among youth with ADHD[17,18] and those with BD-I.[19,20] Alterations in global integration across the brain and in regional interactions among nodes of the default mode network (DMN) and frontoparietal network have been identified among youth with ADHD.[21,22] However, these studies did not control for familial risk of BD or psychostimulant status, and brain connectome features among youth with ADHD with and without familial risk of BD-I have never been systematically investigated.

In the present cross-sectional study, we sought to use a graph-based network analysis of structural magnetic resonance imaging (MRI) data to compare brain network topological properties among psychostimulant-free youth with ADHD with and without a first-degree relative with BD-I, as well as a healthy comparison group. We also sought to evaluate relationships between topological metrics and mood and ADHD symptom ratings. We hypothesized that youth with ADHD with and without a first-degree relative with BD-I would exhibit common structural network abnormalities compared with healthy controls, and that youth with ADHD with a first-degree relative with BD-I would exhibit more extensive topological alterations than those without a first-degree relative with BD-I.

Methods

Participants

We recruited participants from the University of Cincinnati and the local community. We recruited 3 groups of psychostimulant-free youth (aged 10–18 yr), namely youth with ADHD and at least 1 biological parent or sibling with BD-I (high-risk group), youth with ADHD and no first- or second-degree relative with a mood or psychotic disorder (low-risk group) and typically developing healthy controls with no personal or family history of a *Diagnostic and Statistical Manual of Mental Disorders, Fifth Edition* (DSM-5) axis I psychiatric disorder. The Structured Clinical Interview for DSM confirmed a parental diagnosis of BD,[23] and the Family Interview for Genetics Studies (FIGS)[24] was used to confirm DSM-5 diagnoses of BD in first- or second-degree relatives including siblings. Trained clinicians administered diagnostic instruments with established diagnostic reliability ($\kappa > 0.9$). After a complete description of the study, participants and caregivers provided informed assent or consent, respectively.

We excluded youth with MRI contraindications (e.g., braces, claustrophobia), those with an intelligence quotient (IQ) less than 80 as determined by the Wechsler Abbreviated Scale of Intelligence,[25] those with any major medical or neurologic illness that could influence MRI results or any serious episode (> 10 min) of loss of consciousness and those with any lifetime DSM-5 substance use disorder. Youth with ADHD were required to meet DSM-5 criteria for ADHD (all types) using the Kiddie Schedule for Affective Disorders and Schizophrenia;[26] have no current DSM-5 mood, anxiety (other than specific phobias), conduct, eating or psychotic disorders, Tourette disorder, chronic tic disorder or pervasive developmental disorder; have no exposure to psychostimulants (prescription or recreational) or other medications used for the treatment of ADHD (e.g., atomoxetine) for at least 3 months before screening; have no lifetime exposure to mood stabilizers or antipsychotic medications; have no psychotropic medication exposure during the 30 days before screening; and have no clinically important electrocardiogram or blood pressure abnormalities.

Symptom ratings

Ratings of ADHD symptoms were obtained using the clinician-administered Attention-Deficit Hyperactivity Disorder Rating Scale (ADHD-RS-IV).[27] We analyzed inattention and hyperactivity/impulsivity subscale scores separately. Depression symptom severity was determined using the Children's Depression Rating Scale-Revised (CDRS-R),[28] and manic symptom severity was determined using the Young Mania Rating Scale (YMRS).[29] Global functioning was assessed using the Children's Global Assessment Scale (CGAS).[30] Among youth with ADHD, global symptom severity was rated using the Clinical Global Impression-Severity Scale (CGI-S).[31] All clinician ratings were administered by a child and adolescent psychiatrist with established inter-rater reliabilities ($\kappa > 0.9$). Parents completed the Child Behaviour Checklist (CBCL ages 6–18).[32] We assessed the CBCL total score, internalization and externalization subscale scores, and Dysregulation Profile (CBCL-DP) scores (i.e., the sum of the attention, aggression and anxious or depressed subscores).

Image acquisition

We collected high-resolution 3-dimensional T_1-weighted images using a Philips Ingenia 3 Tesla MRI scanner with a 32-channel head coil (repetition time 8.1 ms, echo time 3.7 ms, flip angle 8°, field of view 256 mm × 224 mm, matrix 256 × 224, voxel size 1 × 1 × 1 mm^3, 160 axial slices, gap between slices 0). Foam padding was used to minimize head motion. During scanning, participants lay quietly with eyes closed. Two experienced neuroradiologists inspected images and made decisions about excessive motion artifact; they discarded data with excessive head movements, brain lesions or obvious artifacts.

Data preprocessing

We used SPM12 for preprocessing of the structural images (http://www.fil.ion.ucl.ac.uk/spm). Briefly, we used the unified segmentation model to segment individual structural data to obtain the grey matter images.[33] The resulting grey matter maps were nonlinearly coregistered using Diffeomorphic Anatomic Registration Through Exponentiated Lie Algebra (DARTEL), which involves the iterative calculation of a study-specific template based on the grey matter images from all participants. We then normalized the grey matter images to the Montreal Neurological Institute space in the same space as the brain parcellation. To preserve tissue volume following warping, voxel values in individual grey matter images were modulated by multiplying the Jacobian determinants derived from the normalization. Lastly, we resampled the grey matter data to 2 mm^3 voxels and spatially smoothed voxels using a Gaussian kernel with a full width at half-maximum of 6 mm. Thereafter, we used the smoothed and modulated grey matter image for further analysis.

Structural network construction

In the present study, we defined nodes as brain regions using the automated anatomic labelling (AAL) template, which divides the cerebral cortex and subcortical structures into 90 independent anatomic regions,[34] and then we applied the Kullback–Leibler divergence-based similarity (KLS) method to define interregional connections as edges.[35] The range of KLS is from 0 to 1, where 1 represents an identical distribution for the 2 regions. Specifically, the higher the similarity of grey matter density distribution between 2 anatomic regions, the higher the KLS scores between them, which indicates stronger connections and shorter edges between these regions. We calculated the KLS values between all possible pairs of 90 brain regions, and generated a 90 × 90 similarity matrix for each participant. In this 90 × 90 network matrix, each row and column represents a brain region and each element represents the similarity of morphological distribution of grey matter features between a pair of brain regions.

Network analysis

We used the GRETNA toolbox (http://www.nitrc.org/projects/gretna/) in MATLAB to calculate brain network properties. We applied a wide range of sparsity thresholds (defined as the total number of edges in a graph divided by the maximum possible number of edges) to all correlation matrices, rather than a single threshold. The minimum and maximum sparsity values were chosen to ensure that the thresholded networks were estimable, given the small-world properties of sparse networks, and to ensure that we had the minimum number of spurious edges. We set the range of our sparsity thresholds to 0.10–0.34 with an interval of 0.01.[36] To provide a summarizing scalar value for the selected threshold space, we calculated the area under the curve (AUC) for each network metric across sparsity thresholds to characterize the topological organization of brain features.[37] This measure has proven sensitive in detecting topological alterations of brain networks.[38]

The graph network was represented by the binarized matrix. For each sparsity threshold, we calculated both global and nodal network properties. Global metrics included 5 small-world parameters (characteristic path length, clustering coefficient, normalized clustering coefficient [γ], normalized characteristic path length [λ] and small-worldness [σ]) and 2 network efficiency parameters (global efficiency, local efficiency), all of which reflect the network topological architecture of the whole brain.[39] Metrics pertaining to individual nodes — including nodal degree, nodal efficiency and betweenness — reflect the regional topological centralities.[40] Thus, we obtained a 277-dimensional graphic feature vector, in which the first 7 features were the global metrics and the rest were nodal centrality metrics for the 90 AAL regions.

Statistical analysis

We analyzed demographic and clinical data using SPSS software (IBM SPSS Statistics version 23.0). We used 1-way analysis of variance (ANOVA) and χ^2 tests to compare continuous and categorical variables across groups. We used independent-sample t tests and χ^2 tests to evaluate differences between high-risk and low-risk youth with ADHD. All tests were 2-tailed.

We performed nonparametric permutation tests on the AUC of each network metric to test for between-group differences among the 3 groups. We implemented permutation tests, repeated 10 000 times, with a linear models toolbox in FSL (https://fsl.fmrib.ox.ac.uk/fsl/fslwiki/PALM). We used the 95th percentiles of each distribution as the critical values for significance testing. Using false discovery rate (FDR) correction, we performed post hoc 2-sample comparisons if ANOVA results were significant ($p < 0.05$, FDR corrected).

Exploratory partial correlation analyses determined associations between clinical ratings and those topological metrics found to differ significantly between groups. We performed correlation analyses using SPSS software (IBM SPSS Statistics version 23.0).

Ethics approval

This study was approved by the Institutional Review Board of University of Cincinnati and was registered at clinicaltrials.gov (NCT02478788).

Table 1: Demographic and clinical characteristics

Variable	No. (%) of participants*			p value†	Low-risk youth v. high-risk youth p value‡
	Healthy controls n = 49	Low-risk youth n = 50	High-risk youth n = 50		
Age, yr, mean ± SD	14.60 ± 2.43	14.06 ± 2.53	13.77 ± 2.58	0.251	0.569
Sex, male	30 (61.2)	33 (66.0)	33 (66.0)	0.849	1.000
Handedness, right	47 (96.0)	40 (80.0)	43 (86.0)	0.057	1.000
BMI, mean ± SD	22.53 ± 4.61	23.80 ± 6.76	24.21 ± 7.38	0.402	0.776
Z score	0.56 ± 1.06	0.76 ± 1.19	0.83 ± 1.31	0.532	0.801
Percentile	65.49 ± 29.04	68.34 ± 29.42	70.60 ± 32.57	0.702	0.716
ADHD type					
ADHD-I	–	28 (56.0)	13 (26.0)	–	< 0.001
ADHD-H	–	0 (0.0)	1 (2.0)	–	–
ADHD-C	–	22 (44.0)	36 (72.0)	–	< 0.001
Previous psychostimulant exposure	–	17 (34.0)	23 (46.0)	–	0.221
ADHD-R, mean ± SD					
Total score	3.20 ± 3.93	33.46 ± 10.00	36.00 ± 10.60	< 0.001	0.221
Inattention subscale	1.86 ± 2.27	20.96 ± 4.83	19.98 ± 5.66	< 0.001	0.354
Hyperactivity/impulsivity subscale	1.35 ± 2.10	12.50 ± 8.06	16.02 ± 7.21	< 0.001	0.023
CDRS-R total score, mean ± SD	18.00 ± 2.31	24.04 ± 5.91	27.30 ± 8.18	< 0.001	0.024
YMRS total score, mean ± SD	0.73 ± 1.93	2.98 ± 3.29	5.76 ± 5.67	< 0.001	0.004
CGAS total score, mean ± SD	88.27 ± 5.88	52.60 ± 6.86	50.56 ± 7.26	< 0.001	0.152
CGI-S, mean ± SD	–	4.02 ± 0.55	4.30 ± 0.68	-	0.026
CBCL, mean ± SD					
Total score	6.81 ± 6.55	37.38 ± 18.18	54.17 ± 28.64	< 0.001	< 0.001
Internalizing subscore	2.30 ± 2.40	8.19 ± 6.37	12.74 ± 9.12	< 0.001	0.001
Externalizing subscore	1.49 ± 1.78	8.29 ± 6.83	14.85 ± 12.39	< 0.001	< 0.001
Dysregulation score	2.87 ± 2.85	21.10 ± 9.65	26.34 ± 13.34	< 0.001	0.009

ADHD = attention-deficit/hyperactivity disorder; ADHD-R = Attention-Deficit Hyperactivity Disorder Rating Scale; BMI = body mass index; CBCL = Child Behaviour Checklist; CDRS-R = Children's Depression Rating Scale-Revised; CGAS = Children's Global Assessment Scale; CGI-S = Clinical Global Impression-Severity Scale; SD = standard deviation; YMRS = Young Mania Rating Scale.
*Unless indicated otherwise.
†One-way analysis of variance or χ^2.
‡*t* test or χ^2.

Results

We included 149 youth with a mean age of 14.1 (standard deviation [SD] 2.5) years (36% female), of whom 49 were healthy controls, 50 were low-risk youth with ADHD and 50 were high-risk youth with ADHD. Table 1 summarizes the sociodemographic and clinical characteristics of study participants. There were no significant group differences in age, sex or handedness, or in previous psychostimulant exposure in the ADHD groups. The low-risk group primarily included youth with ADHD-I subtype, and the high-risk group primarily included youth with ADHD-C subtype. There were significant group differences in IQ (healthy controls: mean 106.6, SD 12.8; low-risk group: mean 101.5, SD 12.7; high-risk group: mean 96.4, SD 13.6, $p = 0.001$). Low-risk ($p = 0.048$) and high-risk ($p < 0.001$) groups differed significantly from healthy controls, and high-risk and low-risk groups did not differ ($p = 0.058$). However, IQ was not significantly correlated with any of the altered topological metrics, either within or among groups. All high-risk youth had at least 1 first-degree relative with BD-I, and 5 (10.0%) had 2 first-degree relatives with BD-I. Regarding second-degree relatives, 16 (32.0%) high-risk youth had no second-degree relatives with BD-I, 18 (36.0%) had 1 second-degree relative with BD-I, 9 (18.0%) had 2 second-degree relatives with BD-I, 5 (10.0%) had 3 second-degree relatives with BD-I, 1 (2.0%) had 4 second-degree relatives with BD-I and 1 (2.0%) had 5 second-degree relatives with BD-I; 16 (32.0%) had only 1 first-degree relative and no second-degree relative. For clinical ratings, the high-risk ADHD group exhibited higher scores on the CDRS-R ($p = 0.024$), YMRS ($p = 0.004$), CGI-S ($p = 0.026$), ADHD-R hyperactivity/impulsivity subscale ($p = 0.023$), and higher CBCL Total scores ($p < 0.001$), CBCL Internalizing subscores ($p = 0.001$), CBCL Externalizing subscores ($p < 0.001$) and CBCL Dysregulation scores ($p = 0.009$), than the low-risk ADHD group.

Alterations in brain network properties

We detected significant abnormalities in global network properties across groups, including global efficiency ($p = 0.038$) and characteristic path length ($p = 0.046$). Post

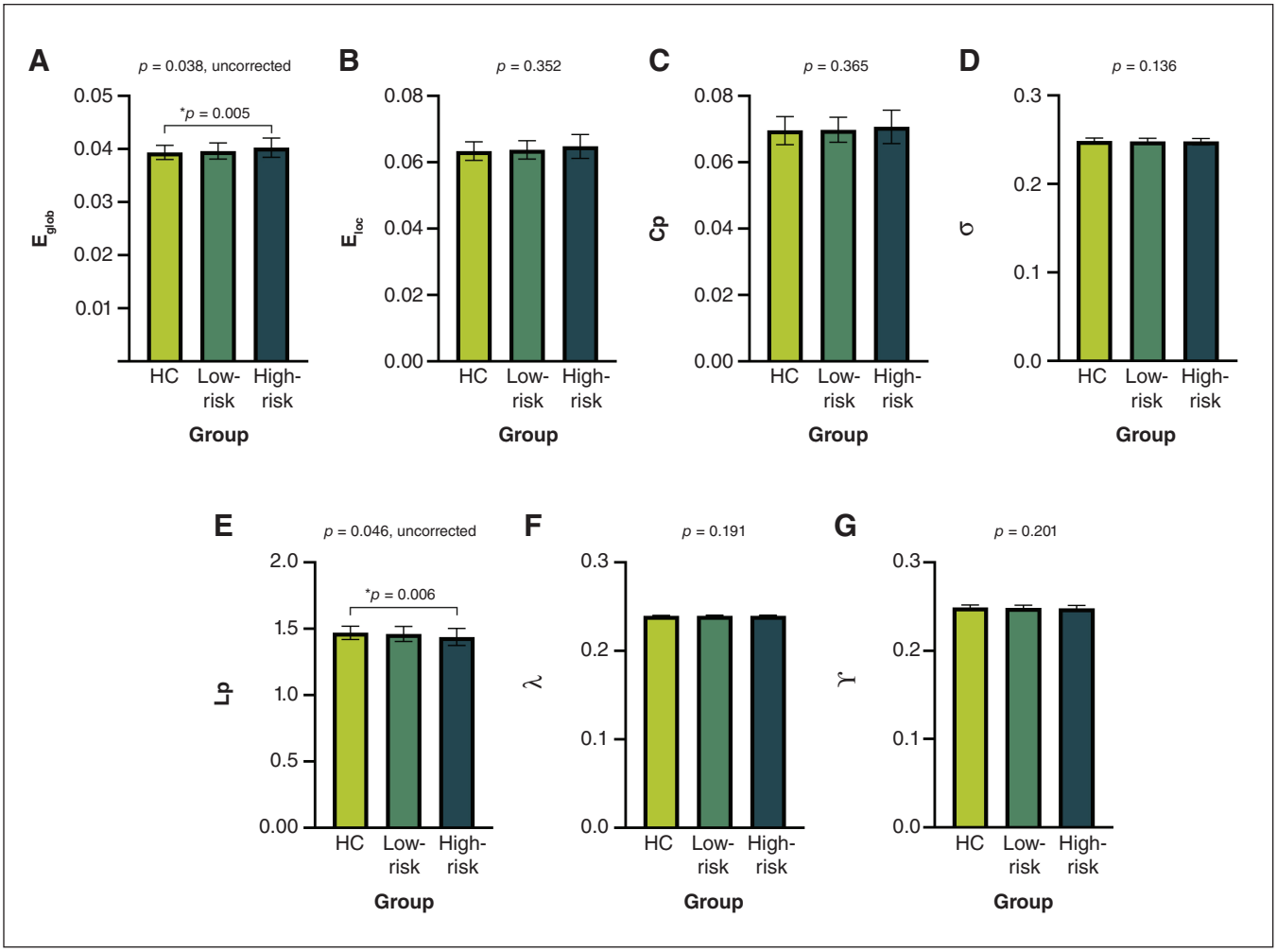

Figure 1: Global topological metrics among high-risk youth with attention-deficit/hyperactivity disorder (ADHD), low-risk youth with ADHD and healthy controls (HC), including (A) global efficiency (E_{glob}), (B) local efficiency (E_{loc}), (C) clustering coefficient (Cp), (D) small-worldness (σ), (E) characteristic path length (Lp), (F) normalized characteristic path length (λ) and (G) normalized clustering coefficient (γ). Presented *p* values are from the analysis of variance; post hoc 2-sample comparisons are corrected by false discovery rate.*HC v. high-risk group.

hoc comparisons showed that only the high-risk group exhibited abnormalities compared with healthy controls, including reduced characteristic path length ($p = 0.006$) and increased global efficiency ($p = 0.005$) (Figure 1). No significant differences were found in other global topological properties.

At the nodal level, we found group differences in topological properties in the left parahippocampal gyrus, right gyrus rectus, right triangular inferior frontal gyrus, right superior parietal gyrus, right opercular inferior frontal gyrus, right rolandic operculum and right inferior occipital gyrus (FDR corrected $p < 0.05$) (Table 2 and Figure 2). Post hoc comparisons showed that both low-risk and high-risk ADHD groups exhibited similar differences compared with healthy controls in the DMN and central executive network (CEN), including decreased nodal metrics in the left parahippocampal gyrus, and increased nodal metrics in the right gyrus rectus, right triangular inferior frontal gyrus and right superior parietal gyrus (FDR corrected $p < 0.05$). The high-risk group exhibited topological alterations in the salience network, including increased nodal metrics in the right opercular inferior frontal gyrus, compared with both the low-risk and control groups (FDR corrected $p < 0.05$).

Relationships between network properties and clinical ratings

Among both low-risk and high-risk ADHD groups ($n = 100$), we found positive correlations between total ADHD-R scores and nodal degree of the right triangular inferior frontal gyrus ($r = 0.22$, $p = 0.028$ uncorrected), and between ADHD hyperactivity/impulsivity subscale scores and nodal degree ($r = 0.34$, $p = 0.001$, uncorrected) and nodal efficiency ($r = 0.27$, $p = 0.008$, uncorrected) of the right triangular inferior frontal gyrus (Figure 3). No significant correlations were found between other global or nodal topological metrics and symptom ratings.

Table 2: Regions with altered nodal centralities

	p value		
Brain region*	Nodal degree	Nodal efficiency	Nodal betweenness
Low-risk v. high-risk v. healthy controls			
Left parahippocampal gyrus (DMN)	0.0015*	0.0037	0.0166
Right gyrus rectus (DMN)	0.0035*	0.0012*	0.2399
Right inferior frontal gyrus, triangular part (CEN)	0.0016*	0.0003*	0.0210
Right superior parietal gyrus (CEN)	0.0033*	0.0014*	0.0209
Right inferior frontal gyrus, opercular part (SN)	0.0074	0.0038	0.0011*
Right rolandic operculum	0.0101	0.0020*	0.2190
Right inferior occipital gyrus	0.0118	0.0035*	0.4445
Low-risk v. healthy controls			
Left parahippocampal gyrus (DMN)	0.0003*↓	0.0010*↓	0.0013*↓
Right gyrus rectus (DMN)	0.0194*↑	0.0175*↑	0.0439
Right inferior frontal gyrus, triangular part (CEN)	0.0148*↑	0.0174*↑	0.0523↑
Right superior parietal gyrus (CEN)	0.0061*↑	0.0089*↑	0.0118*↑
Right rolandic operculum	0.0019*↑	0.0013*↑	0.0430
High-risk v. healthy controls			
Left parahippocampal gyrus (DMN)	0.0076*↓	0.0418*↓	0.0260*↓
Right gyrus rectus (DMN)	0.0001*↑	0.0001*↑	0.1711
Right inferior frontal gyrus, triangular part (CEN)	0.0004*↑	0.0002*↑	0.0018*↑
Right superior parietal gyrus (CEN)	0.0014*↑	0.0008*↑	0.0120*↑
Right inferior frontal gyrus, opercular part (SN)	0.0015*↑	0.0006*↑	0.0002*↑
Right rolandic operculum	0.0055*↑	0.0009*↑	0.1115
Right inferior occipital gyrus	0.0045*↓	0.0008*↓	0.4641
High-risk v. low-risk			
Right inferior frontal gyrus, opercular part (SN)	0.0016*↑	0.0008*↑	0.0003*↑
Right inferior occipital gyrus	0.0075*↓	0.0028*↓	0.1444↓

DMN = default mode network; CEN = central executive network; FDR = false discovery rate; SN = salience network.
*Brain regions were considered abnormal if they exhibited significant differences across groups or between 2 groups ($p < 0.05$, FDR corrected) in at least 1 node centrality parameter (marked by asterisk). All *p* values were obtained using a permutation test. The upward arrow signifies an increase in the measured value of the first group compared to the latter, whereas the downward arrow signifies a decrease in the measured value of the first group compared to the latter.

Discussion

This study investigated structural connectomics among psychostimulant-free youth with ADHD at high risk of BD (with a first-degree relative with BD-I), those at low risk of BD (without a first-degree relative with BD-I) and healthy controls. At the level of global network metrics, high-risk youth with ADHD exhibited a higher global efficiency and lower characteristic path length than healthy youth, while we did not observe global network alterations in the low-risk ADHD group. Direct comparison of the 2 ADHD groups did not identify significant differences in global metrics. At the nodal level, both low-risk and high-risk ADHD groups exhibited similar differences when compared with healthy controls, mainly in the DMN and CEN. We found topological alterations in the salience network between the high-risk group and both the low-risk and healthy control groups. Among low-risk and high-risk ADHD groups, nodal metrics in the right triangular inferior frontal gyrus correlated positively with ADHD-R total scores and ADHD hyperactivity/impulsivity subscale scores. Together, these findings show that familial risk for BD-I, in conjunction with ADHD, is associated with more extensive neuroanatomic connectome alterations, particularly in the salience network, compared with low-risk youth with ADHD, and may represent a prodromal phenotype relevant to risk for developing BD-I.

High-risk youth with ADHD exhibited a higher global efficiency and lower characteristic path length than healthy youth. Global efficiency and characteristic path length are

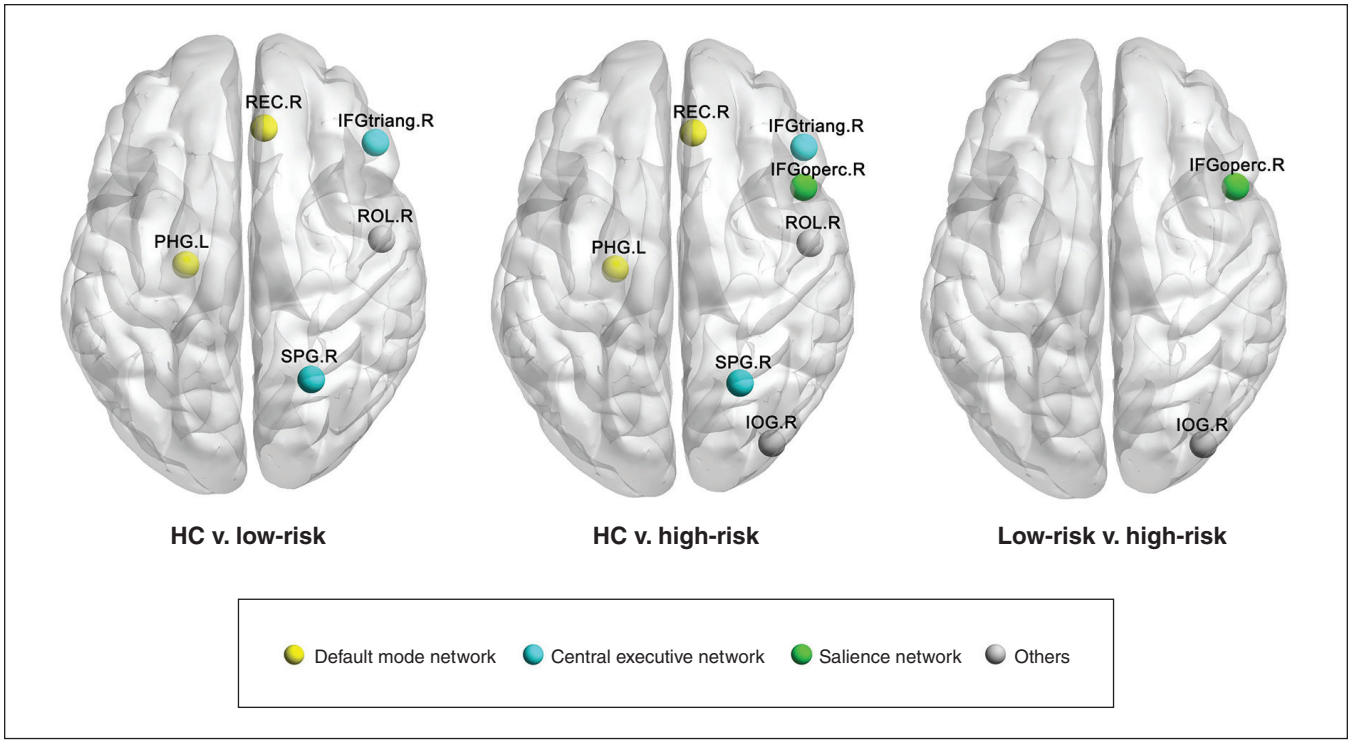

Figure 2: Brain regions exhibiting nodal centrality differences among high-risk youth with attention-deficit/hyperactivity disorder (ADHD), low-risk youth with ADHD and healthy controls (HC). The nodes were mapped onto the cortical surfaces by using the BrainNet Viewer package (www.nitrc.org/projects/bnv). IFGoperc = opercular part of inferior frontal gyrus; IFGtriang = triangular part of inferior frontal gyrus; IOG = inferior occipital gyrus; L = left; PHG = parahippocampalgyrus; R = right; REC = gyrus rectus; ROL = rolandic operculum; SPG = superior parietal gyrus.

measures of global integration and are inversely related.[41] Higher global efficiency indicates stronger network global transmission capability, whereas longer characteristic path length indicates slower network information transmission speed. These results suggest that the brain network of high-risk group has increased integration compared with healthy controls. More specifically, this pattern of global metrics suggests an imbalance between functional segregation and integration, with more efficient information exchange at the global level. In contrast, we did not find any significant differences in global metrics between the low-risk group and healthy youth. Previous graph theory studies have found a less optimized topological organization in global network metrics among youth with ADHD, although the results have been inconsistent.[42–46] For example, some studies have reported increased segregation,[42–44] while others have reported decreased segregation.[45,46] It is important to note, however, that these previous ADHD studies did not control for BD-I familial risk or psychostimulant status, which could account for these discrepancies.

At the node level, we found overlapping abnormalities in the low- and high-risk groups, compared with healthy controls. The nodal metrics of both ADHD groups were generally higher than those of healthy controls, which indicates more efficient information exchange at local levels. Shared nodal metric abnormalities were mainly in the DMN and CEN, which are associated with task-independent introspection[47] and working memory and inhibitory control,[48] respectively. Our findings are in accordance with previous graph-based brain network studies that have found a redistribution of regional nodes and decreased DMN connectivity in ADHD.[21,49] Moreover, attenuated deactivation of the DMN during attention tasks among youth with ADHD has been shown to coincide with attentional lapses.[50] We also observed topological alterations in the CEN; meta-analyses of task-based fMRI studies have consistently found aberrant activation in CEN among people with ADHD compared with healthy controls.[51,52] Evidence from neuroimaging studies further suggest that ADHD is associated with abnormal cortical thinning[53] and altered functional connectivity in the CEN.[54] Overall, our findings support previous evidence implicating disrupted DMN and CEN network organization in ADHD.

In addition to these common abnormalities, the high-risk group exhibited unique topological alterations in the salience network compared with both the low-risk and healthy control groups. The salience network is mainly involved in interoceptive–autonomic processing and mediates the switch between the DMN and CEN.[55] The salience network manages dynamic interactions between the CEN and DMN, and its disruption could interfere with allocating attentional resources to task-relevant information and could impair suppressing responses and disengaging attention from distracting information.[56] Salience network regions in the inferior frontal gyrus, putamen and pallidum are key cortical hubs in circuits that support emotional and cognitive control, and their alterations

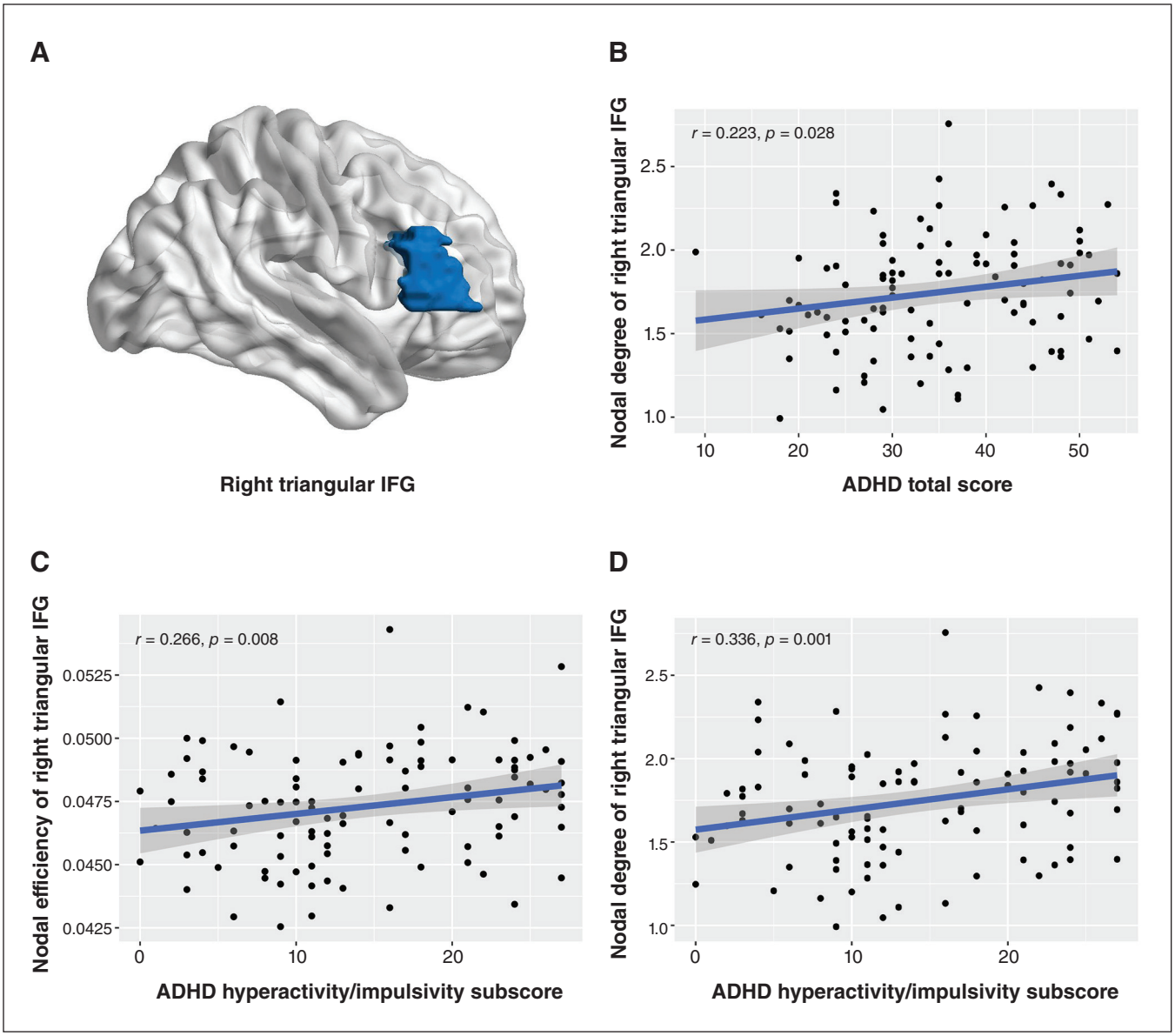

Figure 3: (A) Localization of the right triangular inferior frontal gyrus (IFG). Correlations between nodal metrics in the right triangular IFG and ratings of attention-deficit/hyperactivitiy disorder (ADHD) scores on the ADHD Rating Scale (ADHD-R), including (A) nodal degree and ADHD total score (B) nodal efficiency and ADHD hyperactivity/impulsivity subscale score and (C) nodal degree and ADHD hyperactivity/impulsivity subscale score among both low-risk and high-risk ADHD groups.

have been frequently associated with BD-I.[57,58] Previous research also suggests a potential role of the inferior frontal gyrus in the genetic risk and phenotypic expression of BD-I.[59] Together these findings suggest that changes in topological properties in the salience network are unique to youth with ADHD who have familial risk of BD-I, and may therefore represent a prodromal feature that confers increased risk for developing BD-I.

Our study also found a higher prevalence of ADHD-C among high-risk youth with ADHD, whereas ADHD-I was more common among low-risk youth. This observation is consistent with previous studies that have found higher rates of combined-type ADHD among youth and adults with both BD and ADHD, compared with ADHD alone.[60,61] Moreover, the high-risk group exhibited significantly higher scores on the ADHD hyperactivity/impulsivity subscale, CDRS-R, YMRS, CGI-S, CBCL and CBCL subscales, compared with the low-risk group. Furthermore, score on the ADHD hyperactivity/impulsivity subscale correlated positively with node degree and efficiency in the right triangular inferior frontal gyrus among both low-risk and high-risk ADHD groups. These results suggest that higher nodal degree and efficiency of the right triangular inferior frontal gyrus are related to the more severe hyperactivity/impulsivity symptoms, which is consistent with previous evidence implicating the right inferior frontal gyrus in

response inhibition.[62,63] However, nodal metrics in the right triangular inferior frontal gyrus did not differ between low-risk and high-risk ADHD groups, suggesting that it cannot wholly account for the higher scores on the ADHD hyperactivity/impulsivity subscale exhibited by the high-risk ADHD group.

Limitations

Although we adopted a widely used parcellation template (i.e., AAL 90) to characterize the large-scale connectivity pattern for the human brain networks, other segmentation strategies may yield different findings. The construction of individual structural networks was based on neuroanatomic architecture only, and additional studies are needed to evaluate the functional impact of the observed anatomic network alterations. The high-risk group comprised a greater number of youth with ADHD-C compared with the low-risk group and the observed structural network differences may be related to group differences in ADHD diagnostic subtype rather than familial risk. However, dissociating the contribution of familial risk and ADHD diagnostic subtype to the current findings would require a larger sample size of high-risk youth with an ADHD-I diagnosis. This study was cross-sectional; prospective longitudinal studies are needed to determine the relevance of these findings to BD-I risk progression.

Conclusion

We found that youth with ADHD, both with and without familial risk for BD-I, exhibit common topological alterations in the DMN and CEN; youth with ADHD and a familial risk for BD-I also exhibit topological alterations in the salience network, which may be relevant to familial risk for developing BD-I. Overall, these findings suggest that familial risk for BD-I, in conjunction with ADHD, is associated with different regional structural network abnormalities compared with ADHD alone, and future prospective studies are warranted to evaluate whether these features confer increased risk for developing BD-I.

Affiliations: From the Huaxi MR Research Center (HMRRC), Department of Radiology, The Center for Medical Imaging, West China Hospital of Sichuan University, Chengdu, China (Zhu, Qin, X. Li, Gong); the Department of Psychiatry and Behavioral Neuroscience, University of Cincinnati College of Medicine, Cincinnati, OH (Zhu, Qin, Tallman, Patino, Fleck, Aghera, Sweeney, McNamara, DelBello); the College of Medical Informatics, Chongqing Medical University, Chongqing, China (Lei); the Research Unit of Psychoradiology, Chinese Academy of Medical Sciences, Chengdu, Sichuan, China (X. Li); the Department of Magnetic Resonance Imaging, the First Affiliated Hospital of Zhengzhou University, Zhengzhou, China (W. Li); the Functional and Molecular Imaging Key Laboratory of Sichuan Province, West China Hospital of Sichuan University, Chengdu, Sichuan, China (Gong); the Department of Radiology, West China Xiamen Hospital of Sichuan University, Xiamen, Fujian, China (Gong).

Competing interests: Rodrigo Patino receives research funding from the National Institutes of Health (NIH), the Patient-Centered Outcomes Research Institute (PCORI), Abbvie, Allergan, Janssen, Johnson & Johnson, Lundbeck, Lilly, Otsuka, Pfizer and Sunovion. Melissa DelBello receives research support from the NIH, PCORI, Acadia, Alkermes, Allergan, Janssen, Johnson & Johnson, Lundbeck, Otsuka, Pfizer, Sage, Sunovion and Vanda. She is also a consultant, on the advisory board or has received honoraria for speaking for Alkermes, Allergan, Assurex, CMEology, Janssen, Johnson & Johnson, Lundbeck, Myriad, Neuronetics, Otsuka, Pfizer, Sage, Sunovion and Supernus. She has received travel support from the American Academy of Child and Adolescent Psychiatry. No other competing interests were declared.

Contributors: Ziyu Zhu, Du Lei, Qiyong Gong, John Sweeney, Robert McNamara and Melissa DelBello conceived and designed the study. Maxwell Tallman, Rodrigo Patino, David Fleck and Veronica Agher acquired the data, which Kun Qin, Xiuli Li and Wenbin Li analyzed. Ziyu Zhu and Du Lei wrote the article, which all authors reviewed. All of the authors revised it critically for important intellectual content, gave final approval of the version to be published and agreed to be accountable for all aspects of the work.

Funding: This study was supported by the National Institute of Mental Health (no. R01 MH097818 to Melissa DelBello and Robert McNamara) and the National Natural Science Foundation of China (no. 81820108018 and 82027808 to Qiyong Gong). Du Lei was supported by the Chongqing Talents Exceptional Young Talents Project. Funding sources had no role in the design and conduct of this study; collection, management, analysis or interpretation of the data; preparation, review or approval of the manuscript; or decision to submit the manuscript for publication.

Data sharing: The data presented in this study are available on request from the corresponding author. Some human data are not publicly available for reasons of data protection.

References

1. Ferrari AJ, Stockings E, Khoo J-P, et al. The prevalence and burden of bipolar disorder: findings from the Global Burden of Disease Study 2013. *Bipolar Disord* 2016;18:440-50.
2. Perlis RH, Dennehy EB, Miklowitz DJ, et al. Retrospective age at onset of bipolar disorder and outcome during two-year follow-up: results from the STEP-BD study. *Bipolar Disord* 2009;11:391-400.
3. Singh MK, DelBello MP, Kowatch RA, et al. Co-occurrence of bipolar and attention-deficit hyperactivity disorders in children. *Bipolar Disord* 2006;8:710-20.
4. Propper L, Sandstrom A, Rempel S, et al. Attention-deficit/hyperactivity disorder and other neurodevelopmental disorders in offspring of parents with depression and bipolar disorder. *Psychol Med* 2021;53:559-66.
5. DelBello MP, Geller B. Review of studies of child and adolescent offspring of bipolar parents. *Bipolar Disord* 2001;3:325-34.
6. Biederman J, Faraone S, Mick E, et al. Attention-deficit hyperactivity disorder and juvenile mania: an overlooked comorbidity? *J Am Acad Child Adolesc Psychiatry* 1996;35:997-1008.
7. Brancati GE, Perugi G, Milone A, et al. Development of bipolar disorder in patients with attention-deficit/hyperactivity disorder: a systematic review and meta-analysis of prospective studies. *J Affect Disord* 2021;293:186-96.
8. Castellanos FX, Lee PP, Sharp W, et al. Developmental trajectories of brain volume abnormalities in children and adolescents with attention-deficit/hyperactivity disorder. *JAMA* 2002;288:1740-8.
9. Li X, Sroubek A, Kelly MS, et al. Atypical pulvinar-cortical pathways during sustained attention performance in children with attention-deficit/hyperactivity disorder. *J Am Acad Child Adolesc Psychiatry* 2012;51:1197-207.
10. Proal E, Reiss PT, Klein RG, et al. Brain gray matter deficits at 33-year follow-up in adults with attention-deficit/hyperactivity disorder established in childhood. *Arch Gen Psychiatry* 2011;68:1122-34.
11. Xia S, Li X, Kimball AE, et al. Thalamic shape and connectivity abnormalities in children with attention-deficit/hyperactivity disorder. *Psychiatry Res Neuroimaging* 2012;204:161-7.

12. Halperin JM, Schulz KP. Revisiting the role of the prefrontal cortex in the pathophysiology of attention-deficit/hyperactivity disorder. *Psychol Bull* 2006;132:560-81.
13. Drobinin V, Slaney C, Garnham J, et al. Larger right inferior frontal gyrus volume and surface area in participants at genetic risk for bipolar disorders. *Psychol Med* 2019;49:1308-15.
14. Jeganathan J, Perry A, Bassett DS, et al. Fronto-limbic dysconnectivity leads to impaired brain network controllability in young people with bipolar disorder and those at high genetic risk. *Neuroimage Clin* 2018;19:71-81.
15. Bullmore ET, Sporns O. Complex brain networks: graph theoretical analysis of structural and functional systems. *Nat Rev Neurosci* 2009;10:186-98.
16. He Y, Chen ZJ, Evans AC. Small-world anatomical networks in the human brain revealed by cortical thickness from MRI. *Cereb Cortex* 2007;17:2407-19.
17. Ahmadlou M, Adeli H, Adeli A. Graph theoretical analysis of organization of functional brain networks in ADHD. *Clin EEG Neurosci* 2012;43:5-13.
18. Celik ZC, Colak C, Di Biase MA, et al. Structural connectivity in adolescent synthetic cannabinoid users with and without ADHD. *Brain Imaging Behav* 2020;14:505-14.
19. Lei D, Li WB, Tallman MJ, et al. Changes in the brain structural connectome after a prospective randomized clinical trial of lithium and quetiapine treatment in youth with bipolar disorder. *Neuropsychopharmacology* 2021;46:1315-23.
20. Wang H, Zhu RX, Dai ZP, et al. Aberrant functional connectivity and graph properties in bipolar II disorder with suicide attempts. *J Affect Disord* 2020;275:202-9.
21. Fair DA, Posner J, Nagel BJ, et al. Atypical default network connectivity in youth with attention-deficit/hyperactivity disorder. *Biol Psychiatry* 2010;68:1084-91.
22. Janssen T, Hillebrand A, Gouw A, et al. Neural network topology in ADHD; evidence for maturational delay and default-mode network alterations. *Clin Neurophysiol* 2017;128:2258-67.
23. First MBJTeocp. *Structured clinical interview for the DSM (SCID)*. 2014:1-6.
24. Blehar MC, DePaulo Jr JR, Gershon ES, et al. Women with bipolar disorder: findings from the NIMH Genetics Initiative sample. *Psychopharmacol Bull* 1998;34:239-43.
25. Wechsler D. *Wechsler abbreviated scale of intelligence*. 1999.
26. Kaufman J, Birmaher B, Brent D, et al. Schedule for affective disorders and schizophrenia for School-Age Children-Present and Lifetime Version (K-SADS-PL): initial reliability and validity data. *J Am Acad Child Adolesc Psychiatry* 1997;36:980-8.
27. Faries DE, Yalcin I, Harder D, et al. Validation of the ADHD rating scale as a clirlician administered and scored instrument. *J Attention Dis* 2001;5:107-15.
28. Poznanski EO, Mokros HB. *Children's depression rating scale, revised (CDRS-R)*. 1996.
29. Young RC, Biggs JT, Ziegler VE, et al. Rating-scale for mania — reliability, validity and sensitivity. *Br J Psychiatry* 1978;133:429-35.
30. Shaffer D, Gould MS, Brasic J, et al. A children's global assessment scale (CGAS). *Arch Gen Psychiatry* 1983;40:1228-31.
31. Guy WJEamfp, CGI. *Clinical global impressions*. 1976.
32. Achenbach T. Rescorla LJRCfC, Youth, and Families. *Manual for the ASEBA school-age forms & profiles: an integrated system of multi-informant assessment*. Burlington (VT): University of Vermont; 2001:1617.
33. Ashburner J, Friston KJ. Unified segmentation. *Neuroimage* 2005;26:839-51.
34. Tzourio-Mazoyer N, Landeau B, Papathanassiou D, et al. Automated anatomical labeling of activations in SPM using a macroscopic anatomical parcellation of the MNI MRI single-subject brain. *Neuroimage* 2002;15:273-89.
35. Kong XZ, Wang X, Huang L, et al. Measuring individual morphological relationship of cortical regions. *J Neurosci Methods* 2014;237:103-7.
36. Zhu Z, Lei D, Qin K, et al. Combining deep learning and graph-theoretic brain features to detect posttraumatic stress disorder at the individual level. *Diagnostics (Basel)* 2021;11:1416.
37. Wang J, Wang L, Zang Y, et al. Parcellation-dependent small-world brain functional networks: a resting-state fMRI study. *Hum Brain Mapp* 2009;30:1511-23.
38. He Y, Dagher A, Chen Z, et al. Impaired small-world efficiency in structural cortical networks in multiple sclerosis associated with white matter lesion load. *Brain* 2009;132:3366-79.
39. Braun U, Plichta MM, Esslinger C, et al. Test-retest reliability of resting-state connectivity network characteristics using fMRI and graph theoretical measures. *Neuroimage* 2012;59:1404-12.
40. Zalesky A, Fornito A, Bullmore ET. Network-based statistic: identifying differences in brain networks. *Neuroimage* 2010;53:1197-207.
41. Braun U, Plichta MM, Esslinger C, et al. Test-retest reliability of resting-state connectivity network characteristics using fMRI and graph theoretical measures. *Neuroimage* 2012;59:1404-12.
42. Beare R, Adamson C, Bellgrove MA, et al. Altered structural connectivity in ADHD: a network based analysis. *Brain Imaging Behav* 2017;11:846-58.
43. Cao Q, Shu N, An L, et al. Probabilistic diffusion tractography and graph theory analysis reveal abnormal white matter structural connectivity networks in drug-naive boys with attention deficit/hyperactivity disorder. *J Neurosci* 2013;33:10676-87.
44. Wang L, Zhu C, He Y, et al. Altered small-world brain functional networks in children with attention-deficit/hyperactivity disorder. *Hum Brain Mapp* 2009;30:638-49.
45. Chen Y, Huang X, Wu M, et al. Disrupted brain functional networks in drug-naive children with attention deficit hyperactivity disorder assessed using graph theory analysis. *Hum Brain Mapp* 2019;40:4877-87.
46. Xia S, Foxe JJ, Sroubek AE, et al. Topological organization of the "small-world" visual attention network in children with attention deficit/hyperactivity disorder (ADHD). *Front Hum Neurosci* 2014;8:162.
47. Sheline YI, Barch DM, Price JL, et al. The default mode network and self-referential processes in depression. *Proc Natl Acad Sci U S A* 2009;106:1942-7.
48. Wager TD, Smith EE. Neuroimaging studies of working memory: a meta-analysis. *Cogn Affect Behav Neurosci* 2003;3:255-74.
49. Griffiths KR, Grieve SM, Kohn MR, et al. Altered gray matter organization in children and adolescents with ADHD: a structural covariance connectome study. *Transl Psychiatry* 2016;6:e947.
50. Hart H, Radua J, Mataix-Cols D, et al. Meta-analysis of fMRI studies of timing in attention-deficit hyperactivity disorder (ADHD). *Neurosci Biobehav Rev* 2012;36:2248-56.
51. Cortese S, Kelly C, Chabernaud C, et al. Toward systems neuroscience of ADHD: a meta-analysis of 55 fMRI studies. *Am J Psychiatry* 2012;169:1038-55.
52. Dickstein SG, Bannon K, Castellanos FX, et al. The neural correlates of attention deficit hyperactivity disorder: an ALE meta-analysis. *J Child Psychol Psychiatry* 2006;47:1051-62.
53. Makris N, Biederman J, Valera EM, et al. Cortical thinning of the attention and executive function networks in adults with attention-deficit/hyperactivity disorder. *Cereb Cortex* 2007;17:1364-75.
54. Icer S, Gengec Benli S, Ozmen S. Differences in brain networks of children with ADHD: Whole-brain analysis of resting-state fMRI. *International Journal of Imaging Systems and Technology* 2019;29:645-62.
55. Seeley WW, Menon V, Schatzberg AF, et al. Dissociable intrinsic connectivity networks for salience processing and executive control. *J Neurosci* 2007;27:2349-56.
56. Menon V, Uddin LQ. Saliency, switching, attention and control: a network model of insula function. *Brain Struct Funct* 2010;214:655-67.
57. Chen CH, Suckling J, Lennox BR, et al. A quantitative meta-analysis of fMRI studies in bipolar disorder. *Bipolar Disord* 2011;13:1-15.
58. DelBello MP, Zimmerman ME, Mills NP, et al. Magnetic resonance imaging analysis of amygdala and other subcortical brain regions in adolescents with bipolar disorder. *Bipolar Disord* 2004;6:43-52.
59. Hajek T, Cullis J, Novak T, et al. Brain structural signature of familial predisposition for bipolar disorder: replicable evidence for involvement of the right inferior frontal gyrus. *Biol Psychiatry* 2013;73:144-52.
60. Millstein RB, Wilens TE, Biederman J, et al. Presenting ADHD symptoms and subtypes in clinically referred adults with ADHD. *J Clin Psychiatry* 1997;2:159-66.
61. Donfrancesco R, Miano S, Martines F, et al. Bipolar disorder comorbidity in children with attention deficit hyperactivity disorder. *Psychiatry Res* 2011;186:333-7.
62. Aron AR, Fletcher PC, Bullmore ET, et al. Stop-signal inhibition disrupted by damage to right inferior frontal gyrus in humans. *Nat Neurosci* 2003;6:115-6.
63. Hoekzema E, Carmona S, Tremols V, et al. Enhanced neural activity in frontal and cerebellar circuits after cognitive training in children with attention-deficit/hyperactivity disorder. *Hum Brain Mapp* 2010;31:1942-50.